

Enhanced DOA Estimation via Hybrid Massive MIMO Receive Array with Switches-based Sparse Architecture

Yifan Li, Feng Shu, *Member, IEEE*, Yaoliang Song, *Senior Member, IEEE*, and Jiangzhou Wang, *Fellow, IEEE*

Abstract—Hybrid massive arrays have been widely used in direction of arrival (DOA) estimation for it can provide larger aperture with lower hardware complexity. However, as the signals received by a hybrid array are compressed by the phase shifter network or the switch network, the degree of freedom (DOF) or spatial resolution of hybrid array is lower than fully-digital (FD) array with same number of antennas. Therefore, we develop a novel sparse hybrid array called switches-based sparse hybrid array (SW-SHA) which by combining nested array and switches-based hybrid array to achieve a huge improvement on DOF over traditional hybrid arrays. Simulations of the spatial spectrums verify that SW-SHA can accurately solve the problem of DOA estimation with the number of signal sources much larger than the number of RF chains. Finally, to further improve the accuracy of DOA estimation for SW-SHA, MMV-SW-SHA is proposed by transforming the single-snapshot co-array signal into MMV form. The simulation results also show that MMV-SW-SHA has better performance than SW-SHA when signal-to-noise ratio (SNR) is low.

Index Terms—Direction-of-arrival (DOA), massive MIMO, hybrid architecture, sparse array, compressed sensing.

I. INTRODUCTION

Direction of arrival (DOA) estimation is a fundamental and important topic in array signal processing. For any uniform linear array (ULA)-based DOA estimations, the larger the number of antennas in the arrays, then the higher the spatial resolution and degree of freedom (DOF) of these estimations can be obtained. Thus, the massive MIMO arrays have been widely used for DOA estimation in recent years for the large aperture [1]. However, as the number of array elements increases, the corresponding hardware and software complexity also significantly increase for the large number of radio frequency (RF) chains and large size data matrices to be processed. Therefore, the hybrid analog and digital (HAD) architectures are proposed to decrease the complexity by compressing the large arrays via phase shifter networks [2] [3]. To further reduce the complexity and power consumption, a new hybrid architecture was proposed in [4], which replaced the phase shifter network in hybrid arrays with a switch network. And [5] also proved that switches-based hybrid arrays have a better trade-off between estimation accuracy and power consumption than hybrid arrays with phase shifter network.

As an M -elements fully-digital (FC) ULA is compressed to a K -chains hybrid array via a phase shifter network or a switch network, where $M > K$, the DOF of this array for DOA estimation is also compressed from $M - 1$ to $K - 1$ in theory. While with the same number of array elements,

the DOF of the sparse arrays is significantly higher than that of the ULA, and classical sparse arrays contain minimum redundancy array (MRA) [6], nested array [7], coprime array [8], etc. Therefore, there have been several papers investigating the combinations of hybrid architectures and sparse arrays to improve the DOF of hybrid arrays. [9] gave a sparse array with fully-connected (FC) architecture [5] called CSA, and the DOF of CSA depends on the relationship between M and K . [10] also proposed a hybrid sparse array for active sensing and [11] analyzed the Cramér-Rao bound (CRB) for hybrid sparse architectures.

As the existing hybrid sparse arrays are mostly with phase shifter networks and to further improve the DOF and DOA estimation accuracy for hybrid sparse arrays, we propose two novel sparse architectures for switches-based hybrid arrays. And our main contributions are summarized as follows:

- 1) SW-SHA is proposed to improve the DOF of hybrid massive arrays. This method utilizes the flexibility of the switch network and generates L different sparse subarrays. By combining all the subarrays, we get an augmented sparse array, its difference co-array is a fully filled ULA and has a much larger DOF than existing methods. In addition, from the simulation results, we can find SW-SHA also has great advantages in DOA estimation accuracy.
- 2) In order to improve the DOA estimation accuracy of SW-SHA, MMV-SW-SHA is proposed by selecting $L-1$ different subarrays from all the L subarrays and form the H -snapshots co-array signal \mathbf{R}_{MMV} . MMV-SW-SHA can transform the single-snapshot signal (10) into multi-snapshots form and without decreasing DOF. Simulation results also show that MMV-SW-SHA has a significant improvement in DOA estimation accuracy at low SNR compared to SW-SHA.

Notation: Matrices, vectors, and scalars are denoted by letters of bold upper case, bold lower case, and lower case, respectively. Signs $(\cdot)^T$, $(\cdot)^*$ and $(\cdot)^H$ represent transpose, conjugate and conjugate transpose. \mathbf{I} and $\mathbf{0}$ denote the identity matrix and matrix filled with zeros. $\text{tr}(\cdot)$ stands for trace operation, \otimes and \circ denotes Kronecker product and Khatri-Rao product. $\lfloor \cdot \rfloor$ denotes round down.

II. SYSTEM MODEL

Consider Q far-field narrowband signals impinging on an M -elements uniform linear array (ULA). The q -th signal

$$\begin{aligned}\tilde{\mathbb{P}}_l &= \{(k_1 - 1)L + l \mid 1 \leq k_1 \leq K_1\} \cup \{(k_2(K_1 + 1) - 1)L + l \mid 1 \leq k_2 \leq K_2\} \\ &= \{l, L + l, \dots, (K_1 - 1)L + l, K_1L + l, (2K_1 + 1)L + l, \dots, (K_2(K_1 + 1) - 1)L + l\}\end{aligned}\quad (6)$$

where $|\mathbb{D}| = L^2K^2$, \mathbb{D}_s and \mathbb{D}_c denote self-difference set and cross-difference set respectively. Arrange the elements in \mathbb{D} from small to large, and get $\mathbb{D} = \{D_1, D_2, \dots, D_{L^2K^2}\}$. By vectorizing (8) and using equation $\text{vec}(\mathbf{ABC}) = (\mathbf{C}^T \otimes \mathbf{A})\text{vec}(\mathbf{B})$, we get

$$\mathbf{r} = \text{vec}(\mathbf{R}_\mathbb{P}) = \left(\tilde{\mathbf{A}}_\mathbb{P}^* \circ \tilde{\mathbf{A}}_\mathbb{P} \right) \mathbf{r}_s + \sigma_v^2 \mathbf{i}_{LK} = \tilde{\mathbf{A}}_\mathbb{D} \mathbf{r}_s + \sigma_v^2 \mathbf{i}_{LK} \quad (10)$$

where $\mathbf{r} \in \mathbb{C}^{L^2K^2 \times 1}$, \circ represents Katri-Rao product and $\tilde{\mathbf{A}}_\mathbb{D} = [\tilde{\mathbf{a}}_\mathbb{P}^*(\theta_1) \otimes \tilde{\mathbf{a}}_\mathbb{P}(\theta_1), \dots, \tilde{\mathbf{a}}_\mathbb{P}^*(\theta_Q) \otimes \tilde{\mathbf{a}}_\mathbb{P}(\theta_Q)] \in \mathbb{C}^{L^2K^2 \times Q}$. $\mathbf{r}_s = [\sigma_1^2, \dots, \sigma_Q^2]^T$ and $\mathbf{i}_K = \text{vec}(\mathbf{I}_K)$.

As (10) can be viewed as a single-snapshot virtual signal, it can be solved by CS-based methods for $Q < L^2K^2$ and the most widely used is on-grid methods. Firstly, given a set of angle grid points $\bar{\boldsymbol{\theta}} = \{\bar{\theta}_1, \dots, \bar{\theta}_Q\}$, where $Q \gg Q$, $\bar{\theta}_{q+1} - \bar{\theta}_q = \Delta\theta$ and this means the subsequent DOA estimation can only take values from $\bar{\boldsymbol{\theta}}$. Then we get a dictionary matrix $\tilde{\mathbf{A}}_\mathbb{D} = [\mathbf{a}_\mathbb{D}(\bar{\theta}_1), \dots, \mathbf{a}_\mathbb{D}(\bar{\theta}_Q)]^T \in \mathbb{C}^{L^2K^2 \times Q}$ and the optimization problem is given by

$$\min_{\bar{\mathbf{r}}_s} \|\bar{\mathbf{r}}_s\|_0 \quad \text{s.t.} \quad \|\mathbf{r} - \tilde{\mathbf{A}}_\mathbb{D} \bar{\mathbf{r}}_s\|_2 \leq \epsilon \quad (11)$$

where $\bar{\mathbf{r}}_s \in \mathbb{C}^{Q \times 1}$ is optimization variable and $\|\bar{\mathbf{r}}_s\|_0 = \{\bar{q} : \bar{\mathbf{r}}_s(\bar{q}) \neq 0\}$ counts the nonzero entries of $\bar{\mathbf{r}}_s$. ϵ is a bound related to noise power σ_v^2 . However, (11) is NP hard to solve, so by introducing LASSO algorithm [14], the objective function (11) is transformed to

$$\min_{\bar{\mathbf{r}}_s} \left[\alpha \|\bar{\mathbf{r}}_s\|_1 + \frac{1}{2} \|\mathbf{r} - \tilde{\mathbf{A}}_\mathbb{D} \bar{\mathbf{r}}_s\|_2 \right] \quad (12)$$

where α is a parameter used to make a trade-off between the reconstruction performance and the sparsity of $\bar{\mathbf{r}}_s$. Obviously, the convex optimization problem (12) can be directly solved by CVX toolbox. In this work, to improve computation efficiency, we use alternating direction method of multipliers (ADMM) algorithm [15] as an alternative method.

B. DOF Analysis

Since the DOF of a sparse array is related to the architecture of its difference co-array, then we first give the following proposition.

Proposition 1: The difference co-array of augmented array \mathbb{P} is a filled ULA.

Proof: According to (6) and (9), the self-difference set for $\tilde{\mathbb{P}}_l$ is defined as $\mathbb{D}_s(l) = \{n_1 - n_2 \mid n_1, n_2 \in \tilde{\mathbb{P}}_l\}$ and select the unique elements from it to form a new set

$$\mathbb{U}_s(l) = \{0, L, 2L, \dots, (K_2(K_1 + 1) - 1)L\}, \quad (13)$$

where $\mathbb{U}_s(l)$ is a symmetric set centered on 0, and the negative part is omitted. It can be seen that $\mathbb{U}_s(l)$ is not related to l , so we get $\mathbb{U}_s(1) = \dots = \mathbb{U}_s(L) = \mathbb{U}_s$. Then the cross-difference for $\tilde{\mathbb{P}}_{l_1}$ and $\tilde{\mathbb{P}}_{l_2}$ is defined as

$\mathbb{D}_c(l_1, l_2) = \{n_1 - n_2 \mid n_1 \in \tilde{\mathbb{P}}_{l_1}, n_2 \in \tilde{\mathbb{P}}_{l_2}\}$, and the positive unique elements are selected

$$\mathbb{U}_c(l_1, l_2) = \{l_2 - l_1, L + l_2 - l_1, \dots, (K_2(K_1 + 1) - 1)L + l_2 - l_1\}, \quad (14)$$

where $1 \leq l_1 < l_2 \leq L$ and $1 \leq l_2 - l_1 \leq L - 1$. Therefore, $\mathbb{U}^+ = \mathbb{U}_s \cup \mathbb{U}_c = \{0, 1, 2, \dots, K_2(K_1 + 1)L - 1\}$ is a filled ULA, i.e. the difference co-array of \mathbb{P} is a filled ULA. ■

On the basis of proposition 1, we select the consecutive unique lags from \mathbb{D} and get the following set

$$\mathbb{U} = \{0, \pm 1, \dots, \pm(K_2(K_1 + 1)L - 1)\}, \quad (15)$$

and $|\mathbb{U}| = 2K_2(K_1 + 1)L - 1$. Then according to [7], we know the DOF of \mathbb{D} is $\text{DOF} = K_2(K_1 + 1)L - 1$. It is evidently that DOF depend on the value of L , so we want to find the maximum L that maximizes it. Then firstly We arrange the elements in \mathbb{P} from small to large as $\mathbb{P} = \{p_1, p_2, \dots, p_{LK}\}$ and $p_{LK} = \tilde{p}_{L,K} = K_2(K_1 + 1)L$. Since the actual aperture of receive array is M , then p_{LK} have to satisfy the condition

$$K_2(K_1 + 1)L \leq M \Rightarrow L \leq \frac{M}{K_2(K_1 + 1)}, \quad (16)$$

and referring to the optimal value of K_1, K_2 [7], we can get the maximum DOF of \mathbb{D} as:

| | K is even | K is odd |
|------------|---------------------------------|--|
| K_1, K_2 | $K_1 = K_2 = K/2$ | $K_1 = (K - 1)/2$ $K_2 = (K + 1)/2$ |
| L_{\max} | $\lfloor 4M/(K^2 + 2K) \rfloor$ | $\lfloor 4M/(K + 1)^2 \rfloor$ |
| DOF | $L(K^2 + 2K)/4 - 1$ | $L(K + 1)^2/4 - 1$ |

and DOF of ordinary K -chains hybrid array is $K - 1$, so SW-SHA has significantly improvement on DOF.

IV. SINGLE-SOURCE ANALYSIS

In the single source case, we can get the simplified CRB expression and obtain useful insights for the DOA estimation with switch-based hybrid architecture. As $Q = 1$, we get $\boldsymbol{\alpha} = [\theta, \sigma_s^2, \sigma_v^2]$, then the covariance matrix of \mathbf{y} is given by

$$\mathbf{R} = \sigma_s^2 \tilde{\mathbf{a}}(\theta) \tilde{\mathbf{a}}^H(\theta) + \sigma_v^2 \mathbf{I}_K, \quad (17)$$

and (34) is simplified to

$$\text{CRB}_\theta = \frac{\sigma_v^2}{2N(\sigma_s^2)^2} \left\{ \text{Re} \left[\dot{\tilde{\mathbf{a}}}^H \boldsymbol{\Pi}_{\tilde{\mathbf{a}}}^\perp \dot{\tilde{\mathbf{a}}} \mathbf{R}^{-1} \tilde{\mathbf{a}} \right] \right\}^{-1} \quad (18)$$

where $\tilde{\mathbf{a}} = \tilde{\mathbf{a}}(\theta)$ and

$$\dot{\tilde{\mathbf{a}}} = \frac{\partial \tilde{\mathbf{a}}(\theta)}{\partial \theta} = \mathbf{D} \tilde{\mathbf{a}}(\theta), \quad (19)$$

where $\mathbf{D} = \text{diag}\{j\pi\tilde{p}_1 \cos\theta, \dots, j\pi\tilde{p}_K \cos\theta\}$. Then we can get

$$\begin{aligned} \dot{\tilde{\mathbf{a}}}^H \boldsymbol{\Pi}_{\tilde{\mathbf{a}}}^\perp \dot{\tilde{\mathbf{a}}} &= \tilde{\mathbf{a}}^H \mathbf{D}^H \left(\mathbf{I}_K - \tilde{\mathbf{a}} (\tilde{\mathbf{a}}^H \tilde{\mathbf{a}})^{-1} \tilde{\mathbf{a}}^H \right) \mathbf{D} \tilde{\mathbf{a}} \\ &= \tilde{\mathbf{a}}^H \mathbf{D}^H \mathbf{D} \tilde{\mathbf{a}} - \frac{1}{K} \tilde{\mathbf{a}}^H \mathbf{D}^H \tilde{\mathbf{a}} \tilde{\mathbf{a}}^H \mathbf{D} \tilde{\mathbf{a}} \\ &= \frac{1}{K} \sum_{k=1}^K (\pi \tilde{p}_k \cos\theta)^2 + \frac{1}{K} \left(\frac{1}{K} \sum_{k=1}^K j\pi \tilde{p}_k \cos\theta \right)^2 \\ &= \frac{\pi^2 \cos^2\theta}{K^3} \left[K^2 \sum_{k=1}^K \tilde{p}_k^2 - \left(\sum_{k=1}^K \tilde{p}_k \right)^2 \right], \end{aligned} \quad (20)$$

where $\tilde{\mathbf{a}}^H \tilde{\mathbf{a}} = K$. And by using Sherman-Woodbury identity [12], $\tilde{\mathbf{a}}^H \mathbf{R}^{-1} \tilde{\mathbf{a}}$ can be further solved as

$$\begin{aligned} \tilde{\mathbf{a}}^H \mathbf{R}^{-1} \tilde{\mathbf{a}} &= \tilde{\mathbf{a}}^H \left(\sigma_v^2 \mathbf{I}_K - \frac{\sigma_s^2 \sigma_v^2}{\sigma_v^2 + \sigma_s^2 \tilde{\mathbf{a}}^H \tilde{\mathbf{a}}} \tilde{\mathbf{a}} \tilde{\mathbf{a}}^H \right) \tilde{\mathbf{a}} \\ &= K \sigma_v^2 - \frac{K^2 \sigma_s^2 \sigma_v^2}{\sigma_v^2 + K \sigma_s^2} \\ &= \frac{K^2 (\sigma_v^2)^2}{\sigma_v^2 + K \sigma_s^2}. \end{aligned} \quad (21)$$

Therefore, CRB_θ can be obtained as

$$\text{CRB}_\theta = \frac{\gamma}{\cos^2\theta} \left[K^2 \sum_{k=1}^K \tilde{p}_k^2 - \left(\sum_{k=1}^K \tilde{p}_k \right)^2 \right]^{-1}, \quad (22)$$

where

$$\gamma = \frac{K \sigma_v^2 + K^2 \sigma_s^2}{2N (\sigma_s^2)^2 \sigma_v^2 \pi^2}. \quad (23)$$

Let $\mathbf{P} = [1, 2, \dots, M]^T$ and $\boldsymbol{\Pi} = \text{diag}\{\mathbf{P}\}$, where $\boldsymbol{\Pi}(m, m) = \mathbf{P}(m)$, $1 \leq m \leq M$. Then define a M -elements selection vector $\boldsymbol{\rho} \in \{0, 1\}^M$, and its relationship with compression matrix \mathbf{W} can be expressed as

$$\boldsymbol{\rho} = \sum_{k=1}^K \mathbf{w}_k, \quad (24)$$

where \mathbf{w}_k is the k -th column of \mathbf{W} . Then the expression of CRB_θ can be transformed to

$$\begin{aligned} \text{CRB}_\theta &= \frac{\gamma}{\cos^2\theta} \left[K^2 \|\mathbf{W}^T \mathbf{P}\|_2^2 - \|\mathbf{W}^T \mathbf{P}\|_1^2 \right]^{-1} \\ &= \frac{\gamma}{\cos^2\theta} \left[K^2 \|\boldsymbol{\Pi} \boldsymbol{\rho}\|_2^2 - \|\boldsymbol{\Pi} \boldsymbol{\rho}\|_1^2 \right]^{-1} \\ &= \frac{\gamma}{\cos^2\theta} \left[K^2 \boldsymbol{\rho}^T \boldsymbol{\Pi}^2 \boldsymbol{\rho} - (\mathbf{P}^T \boldsymbol{\rho})^2 \right]^{-1} \\ &= \frac{\gamma}{\cos^2\theta} \left[K^2 \sum_{m=1}^M (m \rho_m)^2 - \left(\sum_{m=1}^M m \rho_m \right)^2 \right]^{-1} \end{aligned} \quad (25)$$

where ρ_m denotes the m -th element of $\boldsymbol{\rho}$.

Obviously, from the above expression, we can see when the signal power σ_s^2 and noise power σ_v^2 are fixed, regardless of which direction the signal was transmitted, there is an optimal compression matrix \mathbf{W} that can make CRB_θ lowest. So, the minimum CRB_θ can be achieved via solving the following optimization problem

$$\begin{aligned} \max_{\boldsymbol{\rho}} \quad & K^2 \|\boldsymbol{\Pi} \boldsymbol{\rho}\|_2^2 - \|\boldsymbol{\Pi} \boldsymbol{\rho}\|_1^2 \\ \text{s.t.} \quad & \|\boldsymbol{\rho}\|_1 = K, \quad \rho_m \in \{0, 1\} \end{aligned} \quad (26)$$

For a switch-based hybrid array with M -sensors and K -RF chains, there are C_M^K different \mathbf{W} in total that can satisfy the constraint condition in (26).

V. SIMULATION RESULTS

In this section, we evaluate the DOA estimation performance of SW-SHA and MMV-SW-SHA via numerical simulations. And we also introduce nested array [7], Coprime array [8], sub-connected array (SCA) [5] and compressed sparse array (CSA) [9] as comparisons, where nested array and Coprime array are classical sparse arrays, SCA and CSA are hybrid arrays, where CSA has sparse architecture. If not specifically stated, all the sources are assumed to have same power and part of the simulation parameters are set as: $M = 128$, $K = 8$, $N = 1000$, $\alpha = 0.25$ and $\Delta\theta = 1^\circ$.

Fig.3 shows the spatial spectrums of these methods with $Q = 16$, $L = 6$. Under this parameter condition, we can get $\text{DOF}_{\text{SW-SHA}} = \text{DOF}_{\text{MMV-SW-SHA}} = 119$, $\text{DOF}_{\text{CSA}} = 31$, $\text{DOF}_{\text{SCA}} = 7$, $\text{DOF}_{\text{NA}} = 19$ and $\text{DOF}_{\text{CA}} = 15$. Thus, our proposed methods have huge improvement on DOF, whether compared to classical sparse arrays or hybrid architecture-based arrays. And from fig.3, we can see all the 16 sources can be accurately distinguished by SW-SHA and MMV-SW-SHA, this also demonstrates the advantages of our methods in spatial resolution, especially for $Q > K$.

To further validate the DOA estimation accuracy of the proposed methods, Fig.4 gives the curves of RMSE versus SNR with $Q = 1$ and the source direction is random generated as $\theta = -67.131^\circ$. It is obviously that proposed SW-SHA and MMV-SW-SHA have significant improvement in DOA estimation accuracy compared to the benchmarks, especially when $\text{SNR} < -8\text{dB}$. In addition, MMV-SW-SHA has higher accuracy under low SNR condition compared to SW-SHA, which proves that the MMV operation we adopted can further improve the DOA estimation accuracy while ensuring the DOF is unchanged.

VI. CONCLUSION

In this work, SW-SHA method was proposed to improve the DOF of massive hybrid arrays by using K switches to construct an augmented sparse array with fully filled co-array. After analysis, we found that the DOF of SW-SHA is much larger than the traditional K -chains hybrid arrays, and the simulation of spatial spectrums showed that it can accurately distinguish signal sources which number is far beyond K . Then in order to further improve the DOA estimation accuracy of SW-SHA and without reducing the DOF, we proposed the MMV-SW-SHA method to transform the co-array signal of SW-SHA into the multi-snapshots form, and referred to the idea of group LASSO algorithm to solve this DOA estimation problem. The final simulation results also indicated that MMV-SW-SHA has evidently improved the estimation accuracy compared to SW-SHA especially at low SNR.

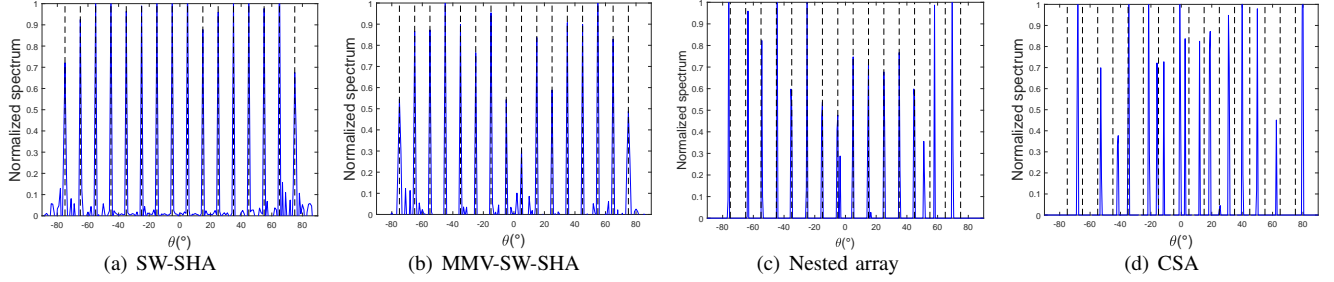


Fig. 3: The spatial spectrums under $Q=16$, $\text{SNR}=0\text{dB}$. (a) SW-SHA with $L=6$, (b) MMV-SW-SHA with $h=4$, (c) K -elements nested array, (d) K -chains CSA.

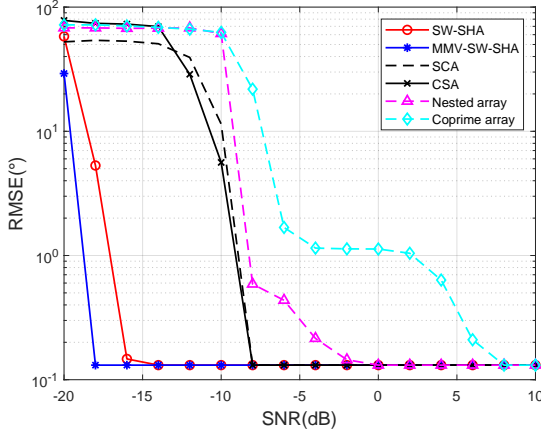


Fig. 4: RMSE versus SNR.

APPENDIX A CRB ANALYSIS

Given a random vector \mathbf{y} with probability density function (PDF) $p(\mathbf{y}; \boldsymbol{\alpha})$, where $\boldsymbol{\alpha}$ is a parameter vector, its fisher information matrix (FIM) is defined as

$$\mathbf{F} = -\mathbb{E} \left\{ \frac{\partial^2 \ln p(\mathbf{y}; \boldsymbol{\alpha})}{\partial \boldsymbol{\alpha} \partial \boldsymbol{\alpha}^T} \right\}, \quad (27)$$

as the observation vector \mathbf{y} in this work follows zero-mean complex Gaussian distribution with covariance matrix \mathbf{R} and the elements in \mathbf{F} can be expressed as

$$\mathbf{F}_{i,j} = \text{tr} \left\{ \mathbf{R}^{-1} \frac{\partial \mathbf{R}}{\partial \alpha_i} \mathbf{R}^{-1} \frac{\partial \mathbf{R}}{\partial \alpha_j} \right\}, \quad 1 \leq i, j \leq 2Q + 1, \quad (28)$$

where $\boldsymbol{\alpha} = [\boldsymbol{\theta}^T, \boldsymbol{\Sigma}^T]$ is a $(2Q + 1) \times 1$ parameter vector, $\boldsymbol{\theta} = [\theta_1, \dots, \theta_Q]^T$ and $\boldsymbol{\Sigma} = [\sigma_1^2, \dots, \sigma_Q^2, \sigma_v^2]^T = [\boldsymbol{\Sigma}_s^T, \sigma_v^2]$. According to the parameter vector, we can get the following partitioned FIM

$$\mathbf{F} = \begin{bmatrix} \mathbf{F}_{\boldsymbol{\theta}\boldsymbol{\theta}} & \mathbf{F}_{\boldsymbol{\theta}\boldsymbol{\Sigma}} \\ \mathbf{F}_{\boldsymbol{\Sigma}\boldsymbol{\theta}} & \mathbf{F}_{\boldsymbol{\Sigma}\boldsymbol{\Sigma}} \end{bmatrix}. \quad (29)$$

Based on the following properties

$$\begin{aligned} (\mathbf{A} \otimes \mathbf{B})^H &= \mathbf{A}^H \otimes \mathbf{B}^H, \\ (\mathbf{A} \otimes \mathbf{B})^{-1} &= \mathbf{A}^{-1} \otimes \mathbf{B}^{-1}, \\ \text{tr}(\mathbf{ABCD}) &= (\text{vec}(\mathbf{B}^H))^H (\mathbf{A}^T \otimes \mathbf{C}) \text{vec}(\mathbf{D}), \end{aligned} \quad (30)$$

and $\mathbf{R}^H = \mathbf{R}$, equation (28) can be transformed to

$$\begin{aligned} \mathbf{F}_{i,j} &= \left(\text{vec} \left(\frac{\partial \mathbf{R}}{\partial \alpha_i} \right) \right)^H (\mathbf{R}^{-T} \otimes \mathbf{R}^{-1}) \text{vec} \left(\frac{\partial \mathbf{R}}{\partial \alpha_j} \right) \\ &= \left(\frac{\partial \mathbf{r}}{\partial \alpha_i} \right)^H (\mathbf{R}^T \otimes \mathbf{R})^{-1} \frac{\partial \mathbf{r}}{\partial \alpha_j} \\ &= \left[(\mathbf{R}^T \otimes \mathbf{R})^{-1/2} \frac{\partial \mathbf{r}}{\partial \alpha_i} \right]^H \left[(\mathbf{R}^T \otimes \mathbf{R})^{-1/2} \frac{\partial \mathbf{r}}{\partial \alpha_j} \right], \end{aligned} \quad (31)$$

where $\mathbf{r} = \text{vec}(\mathbf{R})$. Therefore, the partitioned FIM can be further expressed as

$$\mathbf{F} = \begin{bmatrix} \mathbf{F}_{\boldsymbol{\theta}}^H \\ \mathbf{F}_{\boldsymbol{\Sigma}}^H \end{bmatrix} \begin{bmatrix} \mathbf{F}_{\boldsymbol{\theta}} & \mathbf{F}_{\boldsymbol{\Sigma}} \end{bmatrix} = \begin{bmatrix} \mathbf{F}_{\boldsymbol{\theta}}^H \mathbf{F}_{\boldsymbol{\theta}} & \mathbf{F}_{\boldsymbol{\theta}}^H \mathbf{F}_{\boldsymbol{\Sigma}} \\ \mathbf{F}_{\boldsymbol{\Sigma}}^H \mathbf{F}_{\boldsymbol{\theta}} & \mathbf{F}_{\boldsymbol{\Sigma}}^H \mathbf{F}_{\boldsymbol{\Sigma}} \end{bmatrix} \quad (32)$$

where

$$\begin{aligned} \mathbf{F}_{\boldsymbol{\theta}} &= (\mathbf{R}^T \otimes \mathbf{R})^{-1/2} \frac{\partial \mathbf{r}}{\partial \boldsymbol{\theta}^T}, \\ \mathbf{F}_{\boldsymbol{\Sigma}} &= (\mathbf{R}^T \otimes \mathbf{R})^{-1/2} \frac{\partial \mathbf{r}}{\partial \boldsymbol{\Sigma}^T} \\ &= (\mathbf{R}^T \otimes \mathbf{R})^{-1/2} \left[\frac{\partial \mathbf{r}}{\partial \boldsymbol{\Sigma}_s^T} \middle| \frac{\partial \mathbf{r}}{\partial \sigma_v^2} \right]. \end{aligned} \quad (33)$$

CRB is defined as the inverse of FIM, and we are only interested in the estimation accuracy of $\boldsymbol{\theta}$, so according to derivation in [16], we can get

$$\begin{aligned} \text{CRB}_{\boldsymbol{\theta}} &= \frac{1}{N} (\mathbf{F}_{\boldsymbol{\theta}}^H \boldsymbol{\Pi}_{\boldsymbol{\Sigma}} \mathbf{F}_{\boldsymbol{\theta}})^{-1} \\ &= \frac{\sigma_v^2}{2N} \left\{ \text{Re} \left[\left(\dot{\mathbf{A}}^H \boldsymbol{\Pi}_{\mathbf{A}} \dot{\mathbf{A}} \right) \odot \left(\mathbf{R}_s \tilde{\mathbf{A}}^H \mathbf{R}^{-1} \tilde{\mathbf{A}} \mathbf{R}_s \right) \right] \right\}^{-1}, \end{aligned} \quad (34)$$

where

$$\boldsymbol{\Pi}_{\boldsymbol{\Sigma}} = \mathbf{I}_{K^2} - \mathbf{F}_{\boldsymbol{\Sigma}} (\mathbf{F}_{\boldsymbol{\Sigma}}^H \mathbf{F}_{\boldsymbol{\Sigma}})^{-1} \mathbf{F}_{\boldsymbol{\Sigma}}^H, \quad (35a)$$

$$\boldsymbol{\Pi}_{\mathbf{A}} = \mathbf{I}_K - \tilde{\mathbf{A}} \left(\tilde{\mathbf{A}}^H \tilde{\mathbf{A}} \right)^{-1} \tilde{\mathbf{A}}^H, \quad (35b)$$

$$\dot{\mathbf{A}} = \frac{\partial \tilde{\mathbf{A}}}{\partial \boldsymbol{\theta}^T} = \left[\frac{\partial \tilde{\mathbf{a}}(\theta_1)}{\partial \theta_1}, \dots, \frac{\partial \tilde{\mathbf{a}}(\theta_Q)}{\partial \theta_Q} \right]. \quad (35c)$$

REFERENCES

- [1] R. W. Heath, N. Gonzalez-Prelcic, S. Rangan, W. Roh, and A. M. Sayeed, "An overview of signal processing techniques for millimeter wave mimo systems," *IEEE J. Sel. Topics Signal Process.*, vol. 10, no. 3, pp. 436–453, 2016.
- [2] S.-F. Chuang, W.-R. Wu, and Y.-T. Liu, "High-resolution AoA estimation for hybrid antenna arrays," *IEEE Trans. Antennas Propag.*, vol. 63, no. 7, pp. 2955–2968, 2015.

- [3] F. Sahrabi and W. Yu, "Hybrid digital and analog beamforming design for large-scale antenna arrays," *IEEE J. Sel. Topics Signal Process.*, vol. 10, no. 3, pp. 501–513, 2016.
- [4] R. Méndez-Rial, C. Rusu, N. González-Prelcic, A. Alkhateeb, and R. W. Heath, "Hybrid mimo architectures for millimeter wave communications: Phase shifters or switches?" *IEEE Access*, vol. 4, pp. 247–267, 2016.
- [5] R. Zhang, B. Shim, and W. Wu, "Direction-of-arrival estimation for large antenna arrays with hybrid analog and digital architectures," *IEEE Trans. Signal Process.*, vol. 70, pp. 72–88, 2021.
- [6] A. Moffet, "Minimum-redundancy linear arrays," *IEEE Trans. Antennas Propag.*, vol. 16, no. 2, pp. 172–175, 1968.
- [7] P. Pal and P. P. Vaidyanathan, "Nested arrays: A novel approach to array processing with enhanced degrees of freedom," *IEEE Trans. Signal Process.*, vol. 58, no. 8, pp. 4167–4181, 2010.
- [8] P. P. Vaidyanathan and P. Pal, "Sparse sensing with co-prime samplers and arrays," *IEEE Trans. Signal Process.*, vol. 59, no. 2, pp. 573–586, 2010.
- [9] M. Guo, Y. D. Zhang, and T. Chen, "DOA estimation using compressed sparse array," *IEEE Trans. Signal Process.*, vol. 66, no. 15, pp. 4133–4146, 2018.
- [10] R. Rajamäki, S. P. Chepuri, and V. Koivunen, "Hybrid beamforming for active sensing using sparse arrays," *IEEE Trans. Signal Process.*, vol. 68, pp. 6402–6417, 2020.
- [11] A. Koochakzadeh and P. Pal, "Compressed arrays and hybrid channel sensing: A cramer-rao bound based analysis," *IEEE Signal Process. Lett.*, vol. 27, pp. 1395–1399, 2020.
- [12] E. Tuncer and B. Friedlander, *Classical and modern direction-of-arrival estimation*. Academic Press, 2009.
- [13] G. Qin, Y. D. Zhang, and M. G. Amin, "DOA estimation exploiting moving dilated nested arrays," *IEEE Signal Process. Lett.*, vol. 26, no. 3, pp. 490–494, 2019.
- [14] R. Tibshirani, "Regression shrinkage and selection via the lasso," *Journal of the Royal Statistical Society: Series B (Methodological)*, vol. 58, no. 1, pp. 267–288, 1996.
- [15] S. Boyd, N. Parikh, E. Chu, B. Peleato, J. Eckstein *et al.*, "Distributed optimization and statistical learning via the alternating direction method of multipliers," *Foundations and Trends® in Machine learning*, vol. 3, no. 1, pp. 1–122, 2011.
- [16] P. Stoica, E. G. Larsson, and A. B. Gershman, "The stochastic crb for array processing: A textbook derivation," *IEEE Signal Processing Letters*, vol. 8, no. 5, pp. 148–150, 2001.